Potential profiling of the nanometer-scale charge-depletion layer in *n*-ZnO/*p*-NiO junction using photoemission spectroscopy

Yukiaki Ishida[a] and Atsushi Fujimori
Department of Physics, University of Tokyo, Kashiwa, Chiba 277-8561, Japan
and Department of Complexity Science, University of Tokyo, Kashiwa, Chiba 277-8561, Japan

Hiromichi Ohta
Graduate School of Engineering, Nagoya University, Furo-cho, Chikusa-ku, Nagoya 464-8603, Japan
and ERATO-SORST, JST, in Frontier Collaborative Research Center, S2-6F East, Mail Box S2-13,
Tokyo Institute of Technology, 4259 Nagatsuta-cho, Midori-ku, Yokohama 226-8503, Japan

Masahiro Hirano
ERATO-SORST, JST, in Frontier Collaborative Research Center, S2-6F East, Mail Box S2-13,
Tokyo Institute of Technology, 4259 Nagatsuta-cho, Midori-ku, Yokohama 226-8503, Japan

Hideo Hosono
ERATO-SORST, JST, in Frontier Collaborative Research Center, S2-6F East, Mail Box S2-13,
Tokyo Institute of Technology, 4259 Nagatsuta-cho, Midori-ku, Yokohama 226-8503, Japan
and Frontier Collaborative Research Center, S2-6F East, Mail Box S2-13, Tokyo Institute of Technology,
4259 Nagatsuta-cho, Midori-ku, Yokohama 226-8503, Japan

(Received 9 May 2006; accepted 16 August 2006; published online 10 October 2006)

The authors have performed a depth-profile analysis of an all-oxide *p-n* junction diode *n*-ZnO/*p*-NiO using photoemission spectroscopy combined with Ar-ion sputtering. Systematic core-level shifts were observed during the gradual removal of the ZnO overlayer, and were interpreted using a model based on charge conservation. Spatial profile of the potential around the interface was deduced, including the charge-depletion width of 2.3 nm extending on the ZnO side and the built-in potential of 0.54 eV. © *2006 American Institute of Physics*. [DOI: 10.1063/1.2358858]

Oxides are considered to expand the functions of silicon-based devices since they show a variety of magnetic, electric, dielectric, and optical properties. Innovative oxide junction devices such as transparent field-effect transistors,[1–8] UV-light emitters,[9,10] and those using correlated oxides[11–18] have been reported to date. The characteristic width of the charge-depletion region (CDR) at an oxide junction interface becomes as narrow as several nanometers due to the generally high carrier concentrations in carrier-doped oxides.[18] Investigation of such a narrow CDR is nevertheless of primary importance since CDRs are the center of the device functions. In this letter, we show a potential profile study of a *n*-ZnO/*p*-NiO, which is a representative and promising transparent all-oxide *p-n* junction diode for future oxide electronics.[19] Instead of performing a microscopy around the atomically abrupt interface between *n*-ZnO and *p*-NiO, we approached the interface by a depth-profile analysis using x-ray photoemission spectroscopy (XPS) combined with Ar-ion sputtering [Fig. 1(a)]. Since the typical photoelectron escape depth in XPS is a few nanometers,[20] depth dependent analysis with nanometer resolution became possible.[21]

The epitaxial thin film heterostructure of ZnO(0001)/NiO:Li(111)/indium tin oxide (ITO)(111)/yttria-stabilized zirconia (YSZ)(111) was fabricated as described elsewhere.[19] Here, NiO was *p*-type doped with Li to form $Li_xNi_{1-x}O$. ZnO thickness was 10 nm, derived from the interference fringe. Atomically flat surface and interface of the sample were confirmed by atomic force microscope [AFM: Fig. 1(b)] and high-resolution transmission electron microscope [HRTEM: Fig. 1(c)] observations. XPS measurements were performed using a Scienta SES-100 electron analyzer and an x-ray tube of Al $K\alpha$ line ($h\nu$=1486.6 eV). The energy resolution was ~800 meV, and the base pressure was better than 2×10^{-10} Torr. The voltage stability was better than 5 meV during the measurements, which enabled us to determine the energy shifts with an accuracy of ~40 meV albeit the rather low energy resolution of XPS. *In situ* sample etching was performed in the preparation chamber equipped with an ULVAC USG-3 ion gun and an Ar gas inlet. The energy and the incidence angle of the Ar-ion beam (defocused) were set to 500 eV and 85° (grazing incidence), respectively. During the etching, the sample was moved at ~0.5 Hz in the vertical direction to the incidence beam in order to ensure homogeneous etching. All the measurements were performed at room temperatures.

Figure 1(d) shows a series of core-level XPS spectra recorded during the removal of the initially 10 nm thick ZnO overlayer from the ZnO/NiO:Li/ITO/YSZ sample. The binding energies are referenced to the electron chemical potential μ of the sample, as in usual XPS experiments. In the initial stage of sputtering (for sputtering time $t \lesssim 30$ min), one could see signals only from the ZnO overlayer. The line shapes and the energy positions of the Zn $2p_{3/2}$ and O 1*s* core-level spectra hardly changed in this stage, which confirms the reported chemical robustness of ZnO against Ar-ion sputtering.[22] After $t \sim 30$ min, Ni $2p_{3/2}$ signals from the NiO underlayer became visible and grew in its intensity, while that of Zn $2p_{3/2}$ gradually disappeared. The O 1*s* intensity remained nearly unchanged throughout, since oxygens of similar densities are present both in the ZnO overlayer and the NiO underlayer. At $t \simeq 60$ min, we observed an abrupt termination of the growth of the Ni $2p_{3/2}$ core-level intensity.

[a]Electronic mail: ishida@spring8.or.jp

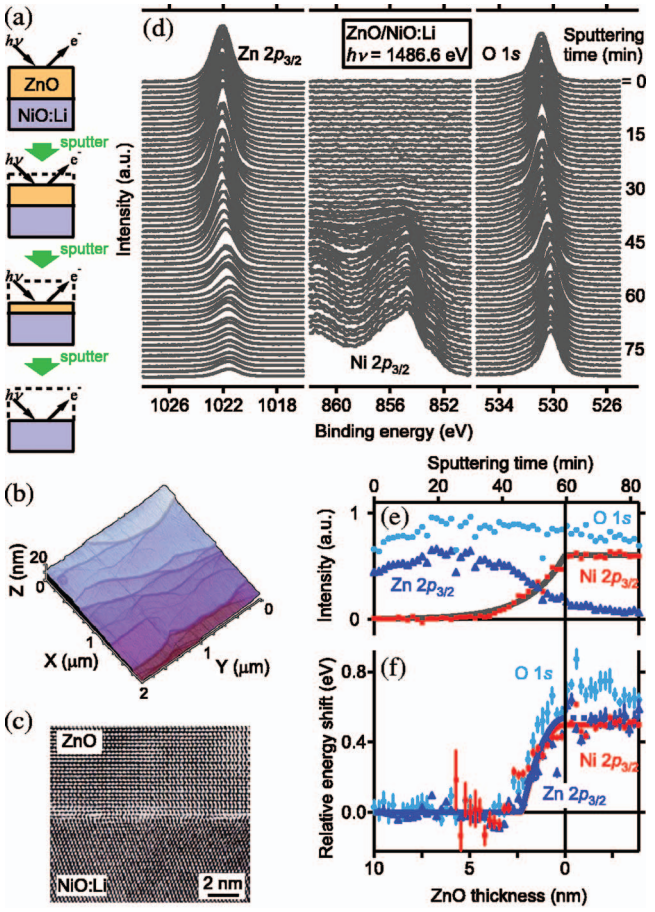

FIG. 1. (Color) Depth-profile analysis of the *n*-ZnO/*p*-NiO:Li junction. (a) Schematic figure of the present experiment. (b) AFM image of a single-crystalline NiO layer grown on an ITO film. (c) HRTEM image of a cross section of the ZnO/NiO heterojunction. (d) Variation of the Zn $2p_{3/2}$, Ni $2p_{3/2}$, and O 1*s* core-level spectra during Ar-ion sputtering. (e) Variation of the core-level XPS intensities as a function of sputtering time. (f) Core-level shifts as a function of sputtering time. Theoretical curves for Zn $2p_{3/2}$ and Ni $2p_{3/2}$, which include the effect of finite photoelectron escape depth, are overlaid.

We interpreted this point as the complete removal of the ZnO layer and the exposure of NiO to the vacuum. Then, from the initial thickness of ZnO and $t \simeq 60$ min, we could accurately determine the sputtering rate of ZnO to be 0.17 nm/min and hence the bottom axis of Figs. 1(e) and 1(f). The exponential rise of the Ni $2p_{3/2}$ intensity for $t < 60$ min was best described by the photoelectron escape depth of 1.9 nm, as shown in the theoretical curve in Fig. 1(e).[23]

In Fig. 1(d), one can also see that the core levels were shifted toward lower binding energies during the etching, most notably in the series of the O 1*s* core-level spectra. The relative shifts of the core levels are plotted in Fig. 1(f). The fitted simulation curves (described below) for the shifts of O 1*s* and Ni $2p_{3/2}$ are also shown. One can clearly see that all the core levels suddenly started to shift toward lower binding energies at $t \simeq 45$ min or, in terms of the ZnO thickness d, at ~ 2.5 nm. The shift continued for further sputtering until the complete removal of ZnO at $t \simeq 60$ min.

The sudden start of the core-level shifts with the kink at $d \sim 2.5$ nm would be understood if we consider the charge conservation in the CDR as follows. Figure 2(a) schematically shows the space-charge distributions within the CDR during the removal of the ZnO overlayer. When part of the CDR on the ZnO side is removed, the CDR on the NiO side

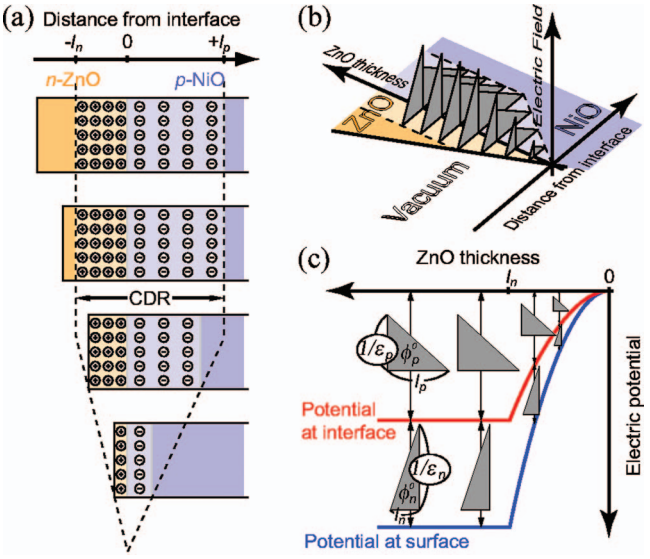

FIG. 2. (Color) Shrink of the CDR of the *p*-*n* junction during the removal process of the ZnO overlayer. (a) Evolution of the charge distribution. (b) Resulting changes in the electric field distributions. (c) Variation in the electronic potential at the exposed surface and interface. The area of the gray triangle in (b) and (c) gives the built-in potential.

should also shrink in order to maintain the charge neutrality. The associated changes in the electric field and electronic potential are schematically shown in Figs. 2(b) and 2(c). After the exposure of the CDR to the vacuum, that is, for $d < l_n$, where l_n is the initial CDR width on the ZnO side, both the built-in potentials in ZnO and NiO (denoted as ϕ_n and ϕ_p, respectively) start to diminish according to $\phi_{n,p} = \phi^0_{n,p}(d/l_n)^2$. Here, ϕ^0_n and ϕ^0_p are the built-in potentials initially formed on the ZnO and NiO sides, respectively. Therefore, as shown in Fig. 2(c), the potential at the surface and interface does not change for $d > l_n$ but suddenly starts to follow parabolas for $d < l_n$.

Roughly speaking, the shift of Zn $2p_{3/2}$ represents the variation in the electronic potential at the surface, since the topmost contribution from the ZnO layer is the largest due to the surface sensitivity of XPS. Similarly, the Ni $2p_{3/2}$ shift represents the potential variation at the interface, since the contribution from the interfacial NiO layer is the largest. The simulated core-level shifts of Zn $2p_{3/2}$ and Ni $2p_{3/2}$ including the photoelectron escape depth of 1.9 nm are overlaid in Fig. 1(f). The best fit was obtained with the parameters $\phi^0_n + \phi^0_p = 0.54$ V (potential shift at the surface), $\phi^0_p = 0.52$ V (potential shift at the interface), and $l_n = 2.3$ nm. The extra shift of the O 1*s* peak compared to Zn $2p_{3/2}$ and Ni $2p_{3/2}$ is understood as the chemical shift in going from ZnO to NiO:Li.

In Fig. 3, we show the band diagram across the *p*-*n* junction thus deduced. Here, the CDR width on the NiO side, $l_p = 1 \times 10^2$ nm, was calculated using the relationship $\varepsilon_n \phi^0_n / \varepsilon_p \phi^0_p = l_n / l_p$, where $\varepsilon_n = 8.59$ (Ref. 24) and $\varepsilon_p = 11.9$ (Ref. 25) are the static dielectric constant ratios of ZnO and NiO, respectively [see Fig. 2(c)]. We have also set the conduction-band minimum of ZnO and the valence-band maximum of NiO:Li close to μ, since ZnO and NiO:Li are heavily doped with electrons and holes, respectively. We adopted the optical gaps of ZnO and NiO of 3.4 and 3.8 eV, respectively,[19] as the band gaps. The built-in potential of $\phi^0_n + \phi^0_p = 0.54$ V is in good agreement with the threshold voltage ~ 0.7 V of the diode rectifying property of *n*-

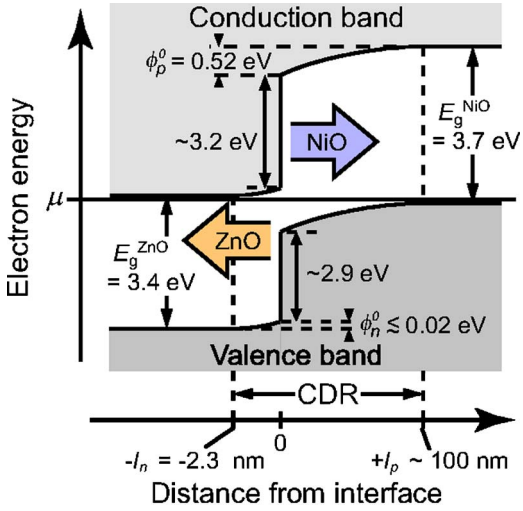

FIG. 3. (Color online) Deduced band diagram at the *n*-ZnO/*p*-NiO:Li interface. Optical band gaps of ZnO and NiO, E_g^{ZnO}=3.4 eV and E_g^{NiO} =3.7 eV, were adopted from the literature (Ref. 19).

ZnO/*p*-NiO.[19] The large conduction-band offset of ~3 eV is in line with the large energy difference in electron affinities of ZnO and NiO.[26]

The carrier concentration of ZnO and NiO:Li can be calculated from the derived parameters as $N_n \sim 3 \times 10^{18}$ cm^{-3} and $N_p \sim 6 \times 10^{16}$ cm^{-3}, respectively, through the relation $N_n l_n = N_p l_p = 2\varepsilon_0 / e(\phi_n^0 + \phi_p^0)/(l_n/\varepsilon_n + l_p/\varepsilon_p)$. Here, ε_0 and e are the dielectric constant of the vacuum and the unit charge, respectively. The derived carrier concentration of ZnO is in reasonable agreement with the initially expected value of $N_n \sim 1 \times 10^{18}$ cm^{-3}.[19] The narrow CDR width of l_n =2.3 nm on the ZnO side, which corresponds to approximately five unit cells of ZnO, stems from the high carrier concentration of ZnO.

So far, spectroscopic studies of the abrupt junction regions with nanometer-to-atomic resolution have been performed using cross-sectional scanning tunneling microscopy and related techniques on cleaved junction cross sections of III-V compound semiconductor heterostructures.[27–29] Thickness dependence analyses as demonstrated here will provide another approach in investigating the nanoscale electronic properties of the junction regions of heterostructures. Since it is not clear how far the simple semiconductor physics is applicable to the interfaces of correlated electron systems,[13,16,18] firm understanding of their interfacial electronic structures would be necessary for further development of oxide junctions.

In summary, we have performed a depth-profile analysis of a *n*-ZnO/*p*-NiO junction using core-level XPS combined with Ar-ion sputtering. During the gradual removal of the ZnO overlayer, an onset of core-level shifts was observed at a critical ZnO thickness ~2.5 nm. We described this behavior using a model based on charge conservation: the CDR shrinks from both sides of the junction when one side of the CDR is mechanically removed. We thus deduced a spatial profile of the potential around the *n*-ZnO/*p*-NiO interface, which is similar to the band diagram of a semiconductor *p*-*n* junction. The present work has demonstrated that the overlayer thickness dependence study can be used as a measure of the applicability of a semiconductor *p*-*n* junction picture to oxide-junction interfaces.

The authors acknowledge Y. Hasegawa, Y. Yuasa, S. Tanaka, and A. Tsuchiya for collaboration, T. Mizokawa for discussion, and K. Nomura, K. Okazaki, H. Wadati, and K. Takubo for technical help. This work was supported by a Grant-in-Aid for Scientific Research in Priority Area "Invention of Anomalous Quantum Materials" from the MEXT, Japan.

[1] M. W. J. Prins, K.-O. Grosse-Holz, G. Müller, J. F. M. Cillessen, J. B. Giesbers, R. P. Weening, and R. M. Wolf, Appl. Phys. Lett. **68**, 3650 (1996).
[2] M. W. J. Prins, S. E. Zinnemers, J. F. M. Cillessen, and J. B. Giesbers, Appl. Phys. Lett. **70**, 458 (1997).
[3] S. Masuda, K. Kitamura, Y. Okumura, S. Miyatake, H. Tabata, and T. Kawai, J. Appl. Phys. **93**, 1624 (2003).
[4] R. Hoffman, B. Norris, and J. Wager, Appl. Phys. Lett. **82**, 733 (2003).
[5] K. Nomura, H. Ohta, K. Ueda, T. Kamiya, M. Hirano, and H. Hosono, Science **300**, 1269 (2003).
[6] K. Nomura, H. Ohta, A. Takagi, T. Kamiya, M. Hirano, and H. Hosono, Nature (London) **432**, 488 (2004).
[7] D. Ginley and C. Bright, MRS Bull. **25**, 15 (2000).
[8] H. Hosono, Int. J. Appl. Ceram. Technol. **1**, 106 (2004).
[9] H. Ohta, K. Kawamura, M. Orita, M. Hirano, N. Sarukura, and H. Hosono, Appl. Phys. Lett. **77**, 475 (2000).
[10] A. Tsukazaki, A. Ohtomo, T. Onuma, M. Ohtani, T. Makino, M. Sumiya, K. Ohtani, S. F. Chichibu, S. Fuke, Y. Segawa, H. Ohno, H. Koinuma, and M. Kawasaki, Nat. Mater. **4**, 42 (2005).
[11] S. Mathews, R. Ramesh, T. Venkatesan, and J. Benedetto, Science **276**, 238 (1997).
[12] C. Ahn, S. Gariglio, P. Paruch, T. Tybell, L. Antognazza, and J.-M. Triscone, Science **284**, 1152 (1999).
[13] H. Tanaka, J. Zhang, and T. Kawai, Phys. Rev. Lett. **88**, 027204 (2002).
[14] Y. Muraoka and Z. Hiroi, J. Phys. Soc. Jpn. **72**, 781 (2003).
[15] H. Katsu, H. Tanaka, and T. Kawai, Appl. Phys. Lett. **76**, 3245 (2000).
[16] A. Tiwari, C. Jin, D. Kumar, and J. Narayan, Appl. Phys. Lett. **83**, 1773 (2003).
[17] A. Sawa, T. Fujii, M. Kawasaki, and Y. Tokura, Appl. Phys. Lett. **86**, 112508 (2005).
[18] C. Ahn, J.-M. Triscone, and J. Mannhart, Nature (London) **424**, 1015 (2003).
[19] H. Ohta, M. Hirano, K. Nakahara, H. Maruta, T. Tanabe, M. Kamiya, T. Kamiya, and H. Hosono, Appl. Phys. Lett. **83**, 1029 (2003).
[20] C. Brundle, J. Vac. Sci. Technol. **11**, 212 (1974).
[21] F. Reniers, in *Handbook of Surface and Interface Analysis, Methods for Problem-Solving*, edited by J. C. Rivière and S. Myhra (Marcel Dekker, New York, 1998), p. 255.
[22] R. Kelly, Nucl. Instrum. Methods **149**, 553 (1978).
[23] The total intensity of the Ni $2p_{3/2}$ photoelectrons emitted from the NiO layer underneath the d nm thick ZnO is $\propto \int_0^\infty e^{-(d+x)/\lambda} dx \propto e^{-d/\lambda}$, where λ is the mean free path of Ni $2p_{3/2}$ photoelectrons.
[24] H. Jaffe and D. Berlincourt, Proc. IEEE **53**, 1372 (1965).
[25] K. V. Rao and A. Smakula, J. Appl. Phys. **36**, 2031 (1965).
[26] H. Hosono and T. Kamiya, Bull. Ceram. Soc. Jpn. **38**, 825 (2003).
[27] E. T. Yu, Chem. Rev. (Washington, D.C.) **97**, 1017 (1997).
[28] P. D. Wolf, R. Stephenson, T. Trenkler, T. Clarysse, T. Hantschel, and W. Vandervorst, J. Vac. Sci. Technol. B **18**, 361 (2000).
[29] H.-K. Lyeo, A. A. Khajetoorians, L. Shi, K. P. Pipe, R. J. Ram, A. Shakouri, and C. K. Shih, Science **303**, 816 (2004).